An In Vivo *Study of Halothane Uptake and Elimination in the Rat Brain with Fluorine Nuclear Magnetic Resonance Spectroscopy*

Lawrence Litt, Ph.D., M.D.,* Ricardo González-Méndez, Ph.D.,† Thomas L. James, Ph.D.,‡ Daniel I. Sessler, M.D.,§ Pam Mills, Ph.D.,† Wil Chew, B.S.,¶ Michael Moseley, Ph.D.,** Brian Pereira, M.D.,†† John W. Severinghaus, M.D.,‡‡ William K. Hamilton, M.D.‡‡

A recent NMR study reported the elimination of halothane from the brain of rabbits to be ten times slower than expected, based on known anesthetic solubility and cerebral blood flow. The authors conducted a study in five rats using fluorine nuclear magnetic resonance (NMR) spectroscopy to see if major pharmacokinetic discrepancies are associated with the uptake, maintenance, and elimination of halothane from the brain. The rats underwent a 60-min period of halothane anesthesia. They employed a spatially selective NMR spectroscopy technique known as surface coil "depth-pulsing" to assure that the fluorine NMR signals originated in brain tissue, and not in the scalp, muscle, adipose tissue, and bone marrow that surround the brain. After the inspired anesthetic concentration was decreased to zero, the amplitude of the fluorine NMR signal decreased to 40% of its maximum value within 34 ± 8.0 minutes (n = 5), rather than after 7 h as in the recent study, where the fluorine signal may have contained substantial contributions from metabolites or tissues outside the brain. Fluorine was barely detectable in all of the animals 90 min after stopping the administration of halothane. The authors' results are in agreement with model calculations and several other investigations. (Key words: Anesthetics, volatile: halothane. Brain: anesthetic uptake and elimination; fluorine. Measurement techniques: nuclear magnetic resonance spectroscopy. Pharmacokinetics.)

This article is accompanied by an editorial. Please see: Smith DS, Chance B: New techniques, new opportunities, old problems. ANESTHESIOLOGY 67:157–160, 1987.

* Assistant Professor of Anesthesia and Radiology; Parker B. Francis Investigator in Anesthesia, 1984–1986.

† Postdoctoral Research Fellow, Department of Anesthesia.

‡ Professor of Chemistry, Pharmaceutical Chemistry and Radiology.

§ Instructor, Department of Anesthesia.

¶ Graduate Student. Department of Pharmaceutical Chemistry.

** Adjunct Assistant Professor of Radiology and Pharmaceutical Chemistry.

†† Research Fellow in Neurosurgery.

‡‡ Professor of Anesthesia.

WYRWICZ *ET AL.* recently demonstrated that ^{19}F nuclear magnetic resonance (NMR) spectroscopy can be used *in vivo* to monitor anesthetic uptake and elimination.[1] In their studies with a 3.5-cm diameter NMR surface coil placed above the heads of 3–4 kg rabbits, they detected the washin and washout of fluorine NMR signals from halothane and some of its metabolites. The authors followed the washin and washout of fluorine NMR signals during and after brief episodes (45–90 min) of halothane anesthesia, and concluded: 1) that the detected ^{19}F NMR signals came *from brain tissue;* 2) that it took approximately 120 min for the halothane signal to fall to one-half of its maximum value; and 3) that approximately 40% of the maximum fluorine signal was present 7 h after the conclusion of a halothane anesthetic.

The halothane washout data of Wyrwicz *et al.* appear to conflict with previous invasive washout studies,[2] model pharmacokinetic calculations,[3–5] and studies of anesthetic solubility.[6] If the elimination of anesthetic vapors from brain tissue is slower than believed, then new clinical concerns arise about prolonged anesthetic action after brief periods of general anesthesia, and new questions arise about molecular interactions of anesthetics with biological tissues.

In general, volatile anesthetics are believed to be freely diffusible substances that aggregate in various hospitable molecular environments (preferably hydrophobic ones), and nonspecifically change macromolecular physical properties.[7,8] The pharmacokinetic assumptions that pertain to current views of anesthetic compartmentation are well described.[3–5,9] Nevertheless, it is tedious to calculate accurate estimates of the anesthetic washout curves for specific organs. Several factors must be known accurately, including cerebral blood flow (which depends upon blood pressure, heart rate, arterial carbon dioxide tensions, and chemical mediators); solubility; cardiac output; the duration of the anesthetic; the pulmonary clearance and minute ventilation; and the relative sizes of the different tissue compartments. An organism undergoing 10 h of halothane anesthesia will have greater body stores of this agent than an organism that underwent 1 hr; and more time

will be required in the first instance to reduce the brain's halothane concentration by 60%. Furthermore, halothane is rapidly metabolized *in vivo*, and the ^{19}F NMR signal from a prominent metabolite, trifluoroacetic acid, has a resonance frequency that is very close to that from halothane,[10] and difficult to resolve *in vivo*.

None of the factors mentioned in the preceeding paragraph leads to a satisfactory explanation of the prolonged presence of the brain halothane NMR signal that was observed by Wyrwicz *et al.* We believe that some or all of the discrepancies between the earlier *in vivo* NMR results and those obtained from invasive biochemical measurements may be attributable to either or both of the following: 1) difficulties in the spatial localization of the *in vivo* ^{19}F NMR signal; and 2) the NMR detection of halothane metabolites. We have, therefore, employed a more volume-selective ^{19}F NMR pulsing technique to measure halothane washin and washout profiles in rats. Our goal was to see if the halothane uptake and elimination behavior in the rat brain is as rapid as expected, or if it is prolonged, as was found by Wyrwicz *et al.* in rabbits.

Although anesthesiologists were recently introduced to some basic NMR concepts in a recent review article on imaging techniques,[11] it seemed to us that further NMR background material would help most readers contemplate the anesthesia-related findings in the studies we are presenting. Accordingly, descriptions of some relevant jargon and physics concepts are contained in an Appendix.

Methods

Anesthesia was induced in five randomly chosen adult Sprague-Dawley rats (350–450 gm) by having them breathe spontaneously in a chamber that contained 4% halothane and oxygen. The animals, which rapidly became unconscious, were turned supine and placed in a 20° Trendelenberg position. When an animal's rate of spontaneous respirations fell to approximately one per second, which was always less then 5 min after anesthesia began, that animal was removed from the chamber for orotracheal intubation under direct vision with a plastic 16-gauge catheter. The non-traumatic laryngoscopy was performed with the aid of a Welsch-Allyn® transilluminator. The time taken to remove the rat from the chamber, position it, and intubate its trachea was always less than 30 s. The endotracheal catheter was secured with paper tape that had no ^{19}F NMR signal. Ventilation was controlled with a Model 683 Harvard® Rodent Respirator that was part of a non-rebreathing ventilation circuit. An intraperitoneal dose of pancuronium (2 mg) was administered immediately after the endotracheal catheter was secured and ventilation was begun. Normal body temperture (39 ± 1° C)

was maintained throughout the experiments. Anesthetic gases were delivered to the circuit from a Fluotec® halothane vaporizer that was calibrated by gas chromatography. Although arterial blood gas measurements were not obtained from rats in this study, the ventilatory pattern that we used (30–40 per minute with adequate chest excursions) has previously resulted[12] in $P_{A_{CO_2}}$ being $\approx$30–40 mmHg.

The inspired halothane concentration was 1% during the first 5 min of controlled ventilation, and then 0.25% for the next 40 min until the wash-in studies began. Supplemental anesthesia for this period was provided by an intraperitoneal dose of ketamine (80 mg/kg) and xylazine (3 mg/kg). During the 40-min period, the animals were positioned prone on a temperature-controlled cradle in a horizontal 5.6 Tesla NMR magnet, with a 12 × 8 mm two-turn elliptical surface coil located above the head, over the brain. Spatially localized *in vivo* NMR spectroscopy was performed using Bendall's "depth-pulse R" for radiofrequency excitations of the brain.[13,14] NMR spectra were constructed by averaging data acquisitions that were obtained every 2 s for 6 min. Each spectrum consisted of 4096 data points. The sweep width for data taking was 16,000 Hz. Signal intensities were obtained by determining the area under the resonance peaks. All signal intensities in a given animal experiment were normalized to the maximum halothane signal for that animal.

Control fluorine NMR spectra for the washin and washout experiments were obtained at the end of the 40-min period of 0.25% halothane anesthesia. The inspired halothane concentration was then increased suddenly to 1%, and brain spectra were obtained every 6 min for 60 min. The halothane vaporizer was then shut off, and 6-min brain spectra were obtained for the next 90 min. The animals were then removed from the spectrometer and allowed to either go back to their cages or more fully recover from the pancuronium injection.

Studies were conducted in two animals that were anesthetized with 1% halothane to see if our NMR "depth-pulse" signals came primarily from the brain. A bilateral tempero-parietal craniectomy was performed, and nearby muscle and scalp tissue were excised so as to leave an area of exposed dura that was $\approx$2.0 × 2.5 cm^2. A small strip of endostial bone was left in place so that the superior sagittal sinus would not be disrupted. A 4 × 6 mm two-turn, elliptical surface coil was then placed directly over the dura. Twelve-minute spectra were collected to explore the changes in the fluorine signal at different depths.

Studies were also performed to measure the longitudinal relaxation time (T_1) of the halothane signal, using a saturation-recovery method.[15,16] The chemical shift of the *in vivo* [19]F halothane signal was compared with that
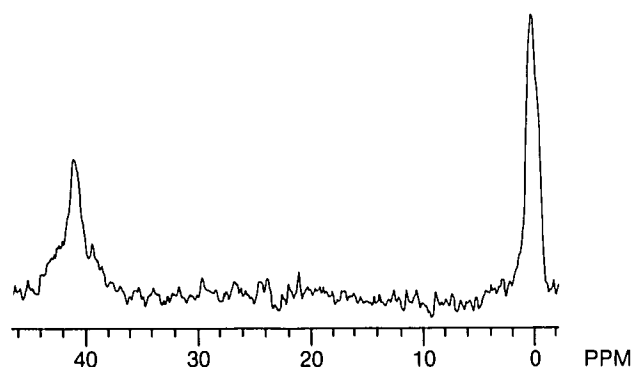
FIG. 1. The *in vivo* fluorine NMR spectrum that was obtained with Bendall's "Depth-Pulse R," as outlined in the text, in one animal. The y direction indicates the NMR signal amplitude, in arbitrary units. The x direction indicates the chemical shift frequency in parts per million units (ppm). The zero point of the x axis has been put at the center of the KF reference signal. The signal from halothane in the animal is seen to be ≈40–42 ppm downfield. Details regarding the signal acquisition are described in the text.
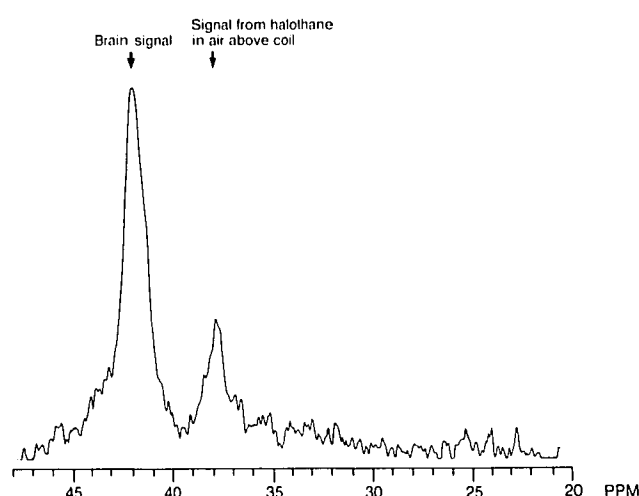

FIG. 2. An NMR spectrum that was obtained under conditions identical to those for figure 1, except that no throat pack or air flow through the magnet bore was used, and halothane gas was allowed to collect inside the magnet. A distinct signal from halothane in the air appears approximately 5 PPM upfield of the brain signal.

of liquid halothane from a commercially available bottle, as well as with those of gaseous halothane. Data are recorded as mean ± SD.

Results

Figure 1 shows the single ^{19}F halothane peak in the NMR spectrum from the head of an anesthetized rat that did not undergo surgery. The "depth-pulse" technique was used to obtain this spectrum. The halothane peak is located ≈42 ppm downfield from the KF reference signal. The T_1 relaxation time of this peak is ≈0.7

± 0.2 s. Figure 2 shows a second peak that will occur close to the one from the brain if halothane is permitted to leak into the air from an uncuffed endotracheal tube and stagnantly collect in the bore of the magnet. This artifactual peak, which is located ≈5 ppm upfield from the biological ^{19}F signal, has been detected in other experiments.[17] It comes from gaseous halothane in the air on the opposite side of the NMR coil from the animal. It can be made to rapidly appear, in the presence or ab-
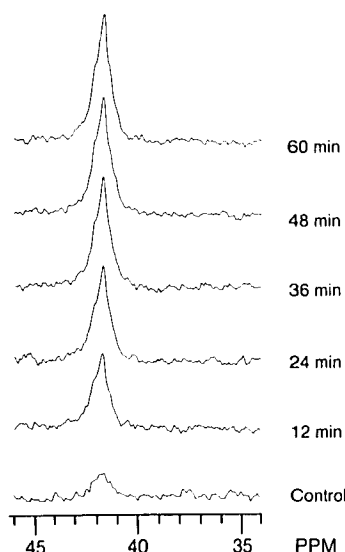
A.

B.

FIG. 3. Six minute *in vivo* ^{19}F NMR spectra obtained from studies of the wash-in (fig. 7A) and wash-out (fig. 7B) in one animal. Successive wash-in (wash-out) spectra are shown above each other. The halothane wash-in data were taken after a sudden change in the inspired halothane concentration from 0.25% to 1.0%. The wash-out data were taken after discontinuing the administration of 1.0% halothane. The data points are plotted at times correspoding to the end of the 6-min data accumulation periods.
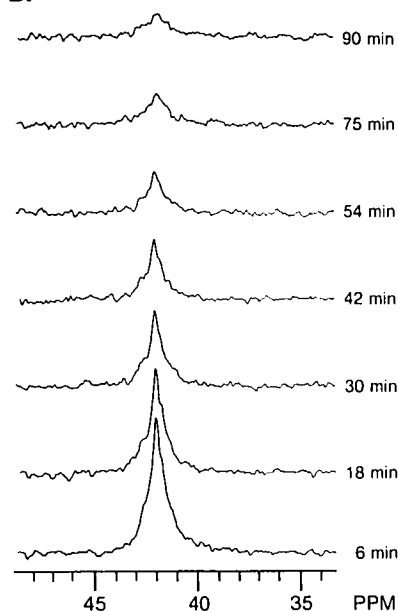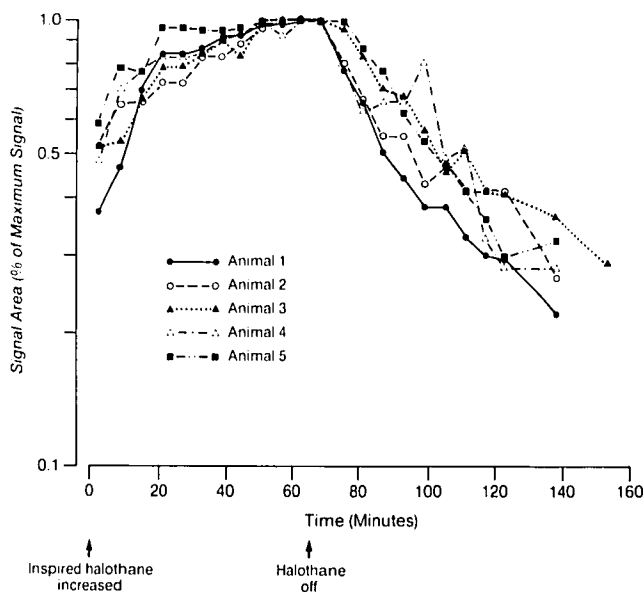
FIG. 4. A semilog plot of the halothane wash-in and wash-out data from the brain, obtained with the "depth-pulse" technique, for five animals. No surgery was performed in these animals, which all recovered after anesthesia. The y-axis (log scale) indicates the integrated NMR signal intensity for the halothane NMR peak, while the x-axis gives the time in minutes. Arrows indicate when the halothane concentration was increased, and then turned off. The intensity of the halothane NMR peak fell to 40% of its maximum value $\approx$ 35 min after halothane was discontinued, rather than $\approx$7 hours afterwards, as in the rabbit experiment by Wyrwicz *et al.*

sence of an animal, by placing an open dish of halothane in the magnet bore. We avoided contamination of our brain halothane signal from unscavenged halothane gas in the bore by flushing it with air.

Halothane was rapidly eliminated from the rat brain after anesthesia. Typical wash-in and wash-out spectra from one animal are shown in figure 3. The data from five animal experiments are shown on the plot in figure 4. No surgery was performed in these five animals, which all recovered uneventfully from their anesthetic at the end of the experiment. Figure 4 demonstrates that a steady-state NMR signal was achieved after $\approx$40 min of wash-in. In the halothane wash-out data, the fluorine peak diminished to 40% of its maximum value in 34.6 ± 8.0 min (n = 5), and no fluorine signal was detectable in any animal 90 min after halothane anesthesia was discontinued. Two straight-line segments were drawn on the semilog plot of the washout curves to obtain estimates for the exponential rate constants for the first two compartments in a simple multi-compartment system: $I = I_1e^{-k_1t} + I_2e^{-k_2t} + \cdots$, where I represents the NMR signal intensity. The resulting estimate for k_1 was (.030 ± .005 min⁻¹), while that for for k_2 was (0.12 ± .003 min⁻¹) (N = 5).
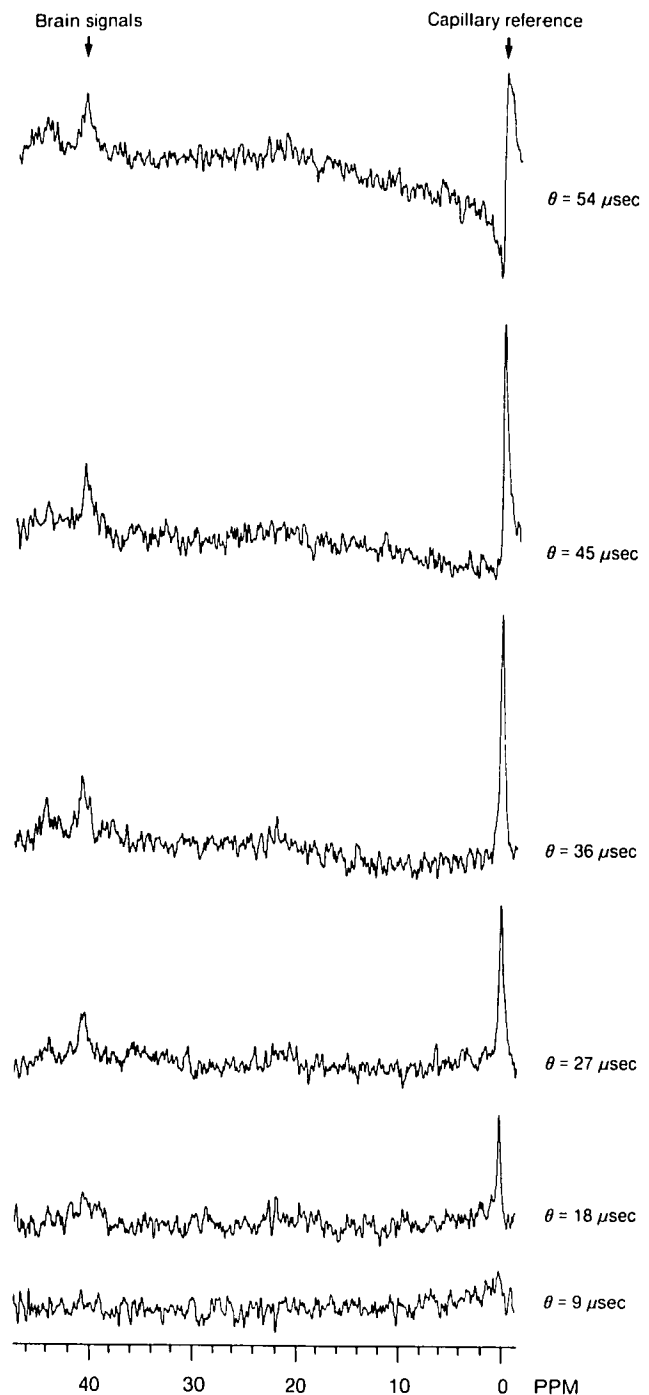

FIG. 5. Spectra demonstrating different depth pulse spectra from the small surface coil that was used in the two craniectomy experiments, which are described in the text. The pulse width parameter, θ (μsec), was increased from its lowest value (bottom tracing) until a 180° inversion was seen in the signal from the reference sample (top tracing). A pulse width parameter that was one-half that needed to produce the 180° flip was chosen. This centered the crescent-shaped detection region at a depth into the brain that was equal to the reference sample's height above the coil. The halothane signal comes entirely from the brain, as described in the text.

Discussion

The uptake, distribution, and metabolism of halothane was elegantly investigated in mice and monkeys by Cohen *et al.* using ^{14}C-labeled autoradiography and radiochromatography.[2,18,19] The studies in monkeys demonstrated that, during the first 2 min of anesthesia, the brain halothane distribution closely paralleled that of the regional cerebral blood flow, with diminished distribution to white matter. After 2 min, there was a slow redistribution of halothane to white matter, areas with heavy myelination and high lipid content. The studies in mice showed that 8% of the brain radioactivity was from metabolites after only 10 min of halothane anesthesia. Fifteen minutes after the halothane was discontinued, 60% of the total brain radioactivity had washed out, and 40% of the remaining radioactivity was from metabolites. Two hours later, the total brain radioactivity was unchanged, but 80% of it came from metabolites. Although the autoradiography studies found that most of the brain halothane was rapidly eliminated after anesthesia, and that some halothane was detectable hours later, no conclusions could be drawn about the relation between anatomic concentration of anesthesia and their effect on brain function.

Our "depth-pulse" wash-out measurements of halothane's cerebral intracellular fluorine signal, which were obtained in healthy rats that fully recovered from anesthesia, are consistent with the washout results of the autoradiographic studies.[2] However, our results are significantly different from those reported in the one-pulse, surface coil NMR studies in rabbits that found $\approx 40\%$ of the total fluorine signal present 7 h after halothane anesthesia was discontinued.[1]

Two phenomena could account for these differences. The first concerns halothane metabolites, which appear within 2 ppm of the *in vivo* halothane peak. Metabolites are known to be in the brain and to contribute to the NMR signal that was detected in the rabbit halothane study at 2.0 Tesla. We did not identify halothane metabolites in our spectra, possibly because the frequency resolution was insufficient, and possibly because the T_1 relaxation time of halothane metabolites at 5.6 Tesla is long compared to the 2-s recycle time. Our NMR signal appears to represent halothane only, and, as such, it is consistent with the ^{14}C autoradiography study.[18]

The second phenomenon concerns contributions to the NMR signal from surrounding tissues with large halothane concentrations. Because the five rats in our study did not have an excision of the underlying scalp, bone, and surrounding muscles, we were concerned about the magnitude of extracerebral contributions to our "depth-pulse" fluorine intensities. To show that halothane in the brain was indeed detectable, we performed NMR studies in two animals with a smaller, less sensitive two-turn elliptical surface coil that was 4 mm $\times$ 6 mm. The two animals had scalp and muscle excisions, and a craniectomy. The halothane signal in figure 5, obtained in one of these experiments, comes entirely from brain tissue, as nothing else was within two coil diameters. We estimate, from imaging techniques that demonstrate the spatial extent of our surface coil excitations,[20] and from our knowledge of the size of the rat cranium, that as much as, but no more than, 20% of the halothane signal in the kinetics experiments comes from sources outside the brain.

In a previous study comparing rats, humans, and whales, the dependence of the rate of anesthetic uptake was correlated with body size.[21] Because the rats that we studied were one-tenth the weight of the rabbits studied by others, one expects rats to have a more rapid anesthetic uptake and elimination. Body size, however, cannot account for a substantially faster reduction of brain halothane in rats as compared to rabbits.

We note that our study design was suboptimal because halothane was administered for 40 min prior to the incremental step in its concentration, and because physiological factors that determine cerebral blood flow were not rigorously controlled. However, the fact that all of the animals recovered indicates that cerebral perfusion was adequate during the experiments. Although the loose control of physiological factors in our experiment could not explain why our NMR signal intensity falls within one-half of an hour to the level seen by Wyrwizc after 7 h, metabolite detection and the detection of extracerebral signals could reconcile the two experiments. It should be noted that our value of k_1, the faster time constant, is in agreement with that obtained by Wyrwicz *et al.* for halothane in rabbits.§§

In conclusion, we find, using the "depth-pulse" technique at 5.6 Tesla, that approximately 80% of the ^{19}F NMR signal amplitude from halothane is gone within 1 h after a 90-min halothane anesthetic. Experiments that detect a significantly larger signal may contain contributions from halothane metabolities, or extracerebral tissues, or both.

Appendix

SHORT REVIEW OF SOME RELEVANT JARGON AND
BASIC PHYSICS CONCEPTS ASSOCIATED WITH
^{19}F IN VIVO NMR SPECTROSCOPY

Although ^{19}F NMR studies of halothane were performed a decade ago in model membrane systems with high resolution

---

§§ Wyrwicz AM, Conboy CB, Nichols BG, Ryback KR, Eisele P: In vivo ^{19}F NMR study of halothane distribution in brain. Biochim Biophys Acta, In Press, 1987
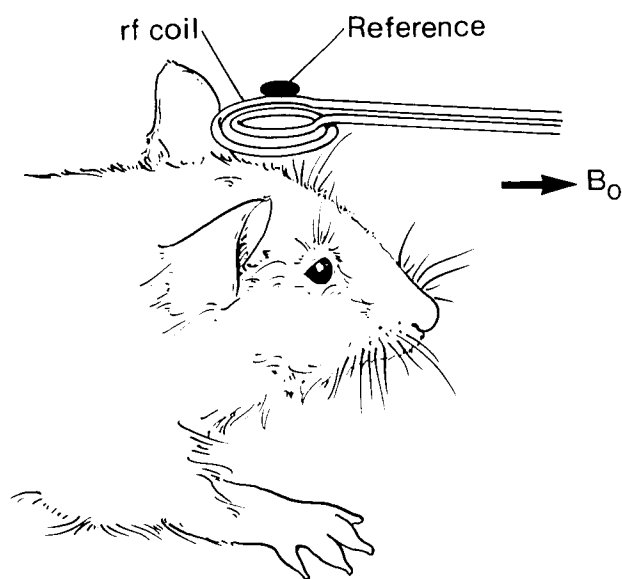
FIG. 6. Schematic diagram showing the external orientation of a two-turn NMR surface coil over the head of a supine rat. The axis of the surface coil is perpendicular to the 5.56 Tesla horizontal magnetic field, which is denoted by B_o. In this study, the NMR reference vial contained a saturated KF solution that was located 5 mm above the coil. A radiofrequency pulse that produces a 90° spin flip in the center of the vial also produces a 90° spin flip at the same depth below the coil, inside the brain.

NMR spectrometers,[10,22] it was only a few years ago that it became possible to obtain the components needed to make large, sophisticated NMR instruments into which animals and humans could fit. The availability of big superconducting magnets, complex high-frequency electronic transmitters and detectors, and elaborate computer systems for controlling and assimilating data has led to the existence of many NMR systems that are being used for *in vivo* spectroscopic studies in animals and humans.[23] While some of the NMR techniques that are used to study molecules dissolved in solution can also be used when performing NMR spectroscopy *in vivo*, many high-resolution NMR methods cannot be used to approach the special technical problems that are unique to *in vivo* NMR studies, especially those arising when the tissue sample under investigation is *in situ* in a human or animal organism.

Substantial progress in ^{19}F NMR techniques has accompanied the advances that took place for proton and phosphorous NMR. *In vivo* ^{19}F NMR images have been made of the intravascular distribution of nondiffusible fluorinated hydrocarbon blood substitutes.[24–26] Surface coil ^{19}F NMR spectroscopy has also been used in *in vivo* animal studies to study the partitioning of halothane into normal tissue and tumor tissue in anesthetized rats,[27] and to study the partitioning of anesthetics in different compartments in excised tissues.[28] More recently, it has been also been shown possible to construct ^{19}F NMR images of animals that are anesthetized with halothane.[29]

Several reviews are available of the fundamental principles of NMR spectroscopy.[30] (When *in vivo* NMR spectroscopy is mentioned in the literature by radiologists, it is usually referred to as *magnetic resonance spectroscopy*, or MRS, just as

magnetic resonance imaging is referred to as MRI.) The basic arrangement, in all cases, is similar to the one that we used to obtain *in vivo* NMR spectroscopy of the brain. This is diagrammed schematically in figure 6, which depicts a rat sitting in a horizontal magnetic field. A specially designed NMR coil is located above the animal's head. A capillary tube containing a selected reference compound, potassium fluoride (KF) in our experiment, is located above the NMR coil.

An NMR spectrum, such as that shown in figure 1, is a plot of signal amplitude *versus* radiofrequency (rf). The vertical axis, in arbitrary units, is proportional to the number of fluorine nuclei per frequency interval that are excited by the rf electromagnetic energy. The horizontal axis gives the chemical shift, δ, or rf frequency relative to a reference frequency, f_{ref}, in parts per million units (ppm). In our experiments, the reference signal originated from fluoride ions, F^-, in the dissociated KF reference solution. The appearance of a sharp peak in the NMR spectrum is called a resonance, and it corresponds to the detection of atomic nuclei that have the same electromagnetic molecular environment. The formal definition of the chemical shift, δ, is given for a peak centered at the frequency f by the formula: $\delta = [(f - f_{ref})/f_{instr}] \times 10^6$; where f_{ref} is the resonance frequency for the arbitrarily chosen reference signal, (fluoride ions in our case, as mentioned above), and f_{instr}, the Larmor frequency for ^{19}F in the spectrometer, is 40.07 MHz/Tesla. Because the horizontal superconducting magnet operates at 5.56 Tesla, a magnetic field approximately 100,000 times that of the earth's, f_{instr} is ≈ 223 MHz. In the *in vivo* NMR spectra presented in this manuscript, each resonance peak represents fluorine nuclei attached to different chemical positions on different molecules. The area under a peak in the spectrum, also referred to as that peak's integrated NMR signal intensity, is proportional to the number of nuclei at the chemical position of interest.

In figure 2, the reference peak on the right arises from fluorine ions in the capillary tube above the animal's head, while the peak on the left comes from the fluorine nuclei in halothane (CF_3-$CHBrCl$) within the brain of the animal. At all magnetic field strengths, the ^{19}F nucleus in halothane resonates at a radiofrequency that is ≈ 42 PPM smaller than that for the ^{19}F nuclei in KF. This significant chemical shift, which arises because the ^{19}F nuclei in halothane experience a magnetic field that is slightly different from the one experienced by fluoride ions, allows halothane to be clearly distinguished. The strongest magnetic field currently used in human NMR spectrometer/imaging systems is 2.0 Tesla. In order to obtain a 5.56 Tesla magnetic field, our magnet was built having a small bore (8.4 cm in diameter), which limits our studies to animals weighing less than 500 gm. However, stronger magnetic fields can result in better NMR signal-to-noise ratios (*i.e.*, in increased NMR sensitivity), so that shorter accumulation times can be employed during physiological studies. In our 5.56 Tesla system, it was possible to obtain ^{19}F brain spectra every 6 min, quickly enough to perform the wash-in and wash-out measurements.

Each NMR resonance peak is further described by two relaxation times, T_1 and T_2, which characterize how long it takes for the longitudinal and transverse magnetization of a perturbed nuclear spin system to return to its equilibrium state by various radiationless mechanisms. T_1 and T_2 are also re-

ferred to as the spin-lattice and spin-spin relaxation times. They depend upon many physical properties, including the magnetic field strength, and can be different for each resonance. Nuclei have shorter relaxation times *in vivo* than in carefully chosen *in vitro* chemical solutions, where only a few compounds besides the one of interest are present. In our NMR experiments, the time delay between rf excitations of the sample was larger than the two relaxation times, while the time duration of the signal measured with the NMR detection coil was smaller. The measured NMR signal intensities were approximately 95% of the value they would have if the spectra had been "fully relaxed," and changes in the NMR signal intensities were always in the same direct proportion to changes in the *in vivo* fluorine concentration.

Nuclear spin distributions are altered, *i.e.* "tipped" or "flipped," when rf current pulses in the transmitter/receiver coil, *i.e.* the two-turn surface coil in our experiment, create a perturbing magnetic field, known as the "B_1 field." The B_1 field from a surface coil has considerably greater spatial variation than the homogeneous B_1 field that is produced by solenoidal and "bird-cage" coils, two kinds commonly used in high-resolution NMR instruments. It is thus more difficult in practice to perform certain types of NMR experiments, because an inhomogeneous B_1 results in different "tip" angles occurring at different locations in space. Some controversy exists as to whether or not surface coils compromise the accuracy of T_1 and T_2 relaxation time measurements. Interestingly, "depth-pulse" schemes, which consist of averages of different cycles of rf excitations, eliminate many of the major problems caused by the inhomogeneous B_1 field.[14]

Several radiofrequency pulsing techniques can be used to acquire spectra.[31,32] The "one-pulse" NMR experiment has been commonly used for *in vivo* studies because of the ease with which it is implemented in a spectrometer. We have used the "one-pulse" method in previous *in vivo* phosphorous studies, and Wyrwicz *et al.* used it in their fluorine studies. However, spatial localization is a serious concern with this technique, which has the NMR signal originating from two regions: a broad one that is centered approximately one radius away from the coil, and a smaller one that is very close to the coil. We recently compared[20] the spatial origin in the "one-pulse" method with that achieved by an alternative pulsing method. In a special study, imaging coils were used together with the same two-turn surface coil that we routinely place outside an organism for the *in vivo* detection of nuclei within the hemispherical region below. The surface coil was used to induce magnetization in a homogeneous chemical solution with the same radiofrequency pulse sequences that are employed *in vivo*. Two pulse sequencing methods were investigated: 1) the standard "one-pulse" NMR experiment; and 2) the "depth-pulse" NMR experiment.[13,14,32] An imaging program was used to make two-dimensional cross-sectional maps of the magnetic excitation that the surface coil pulses induced in the liquid. Figure 7A shows the contour plots that were measured after the standard one-pulse sequence. Each contour line represents a particular signal intensity. The ensemble of contour lines defines two-dimensional histogram bins analogous to those defined by isobaric contours on a topographical map of a mountain range. Within the innermost closed contours in figure 7, the detected signal intensity ranged from
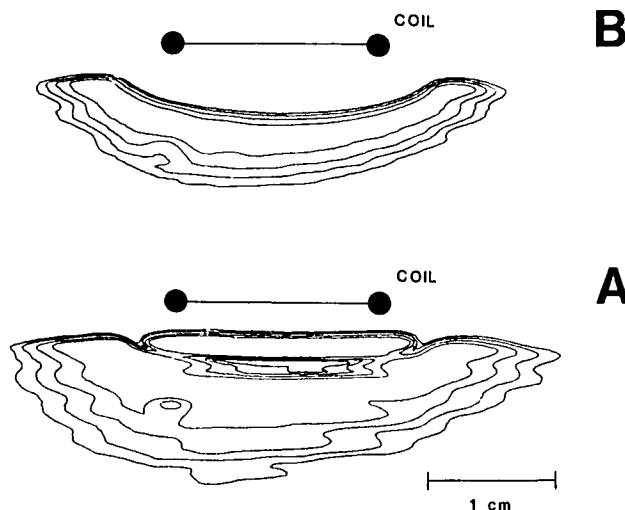

FIG. 7. Two-dimensional, cross-sectional image showing the magnetic excitation measured in a homogeneous liquid underneath a surface coil. The B_o field is perpendicular to the plane of the paper. In figure 7A, a one-pulse sequence was used. In figure 7B, Bendall's Depth Pulse "R" was used. The contours topographically define regions of magnetic strength, as discussed in the text. A thin horizontal region of substantial signal intensity can be seen in figure 7A between the coil and the crescent-shaped region of maximal signal intensity. Reprinted from González-Mendez R, Moseley ME, Murphy-Boesch J, Chew WM, Litt L, James TL: Selective inversion with surface coils. Use of depth pulses for the inversion-transfer experiment in vivo. Journal of Magnetic Resonance 65:516–521, 1985, with permission.

80% of its maximum value to 100%. The successive outer contours define regions where the signal intensity ranges from 60–80%, from 40–60%, etc. Figure 7 shows that the detection efficiency for an NMR surface coil is different in the various regions defined in the contour plots. The regions that are seen with the imaging coils to have larger signal intensities contribute more to the signal in the surface coil experiments. The contours shown also allow an estimation of the detection volume. It can be seen in the cross-sectional view displayed in figure 7A that the edges of the detection volume are "fuzzy" in the one-pulse NMR experiment, and that there are two regions of high acceptance for the nuclear signal: the well-known crescent-shaped one that is approximately one radius below the coil; and a second smaller region that is closer to the coil.[19] Figure 7B showns that, when Bendall's "depth pulse" technique is applied,[13,14,32] the spatial localization is substantially improved. The contours in figure 7B, which were measured after the use of the "depth-pulse" sequence, show only one region of high signal intensity. There is no longer a large signal from a region near the plane of the coil, as in the one-pulse sequence. The closed contour that is obtained with the "depth-pulse" method is also smaller than the one obtained with the one-pulse method. We therefore employed the "depth-pulse" technique during our ^{19}F NMR studies, in order to minimize signal contributions from peripheral regions outside the brain.

Figure 7 also demonstrates that one must also be concerned about the size and location of one's external NMR detection coil. Although the peripheral region of the coil's detection

volume may have a lower detection sensitivity, a large signal amplitude could originate from the periphery if subcutaneous adipose tissue or bone marrow fat were located there. Because bone marrow and fat can each have halothane concentrations that are approximately 20 times that in the brain, it is conceivable that half of the fluorine NMR signal might arise from tissues in close proximity to the brain, where the NMR detection sensitivity is only 5% of that in the brain.

References

1. Wyrwicz AM, Pszenny MH, Schofield JC, Tillman PC, Gordon RE, Martin PA: Noninvasive observations of fluorinated anesthetics in rabbit brain by fluorine-19 nuclear magnetic resonance. Science 222:428–430, 1983

2. Cohen EN, Hood N: Application of low-temperature autoradiography to studies of the uptake and metabolism of volatile anesthetics in the mouse: III. Halothane. ANESTHESIOLOGY 31:553–559, 1969

3. Fukui Y, Smith NT: Interactions among ventilation, the circulation, and the uptake and distribution of halothane—Use of a hybrid computer mulitple model: I. The basic model. ANESTHESIOLOGY 54:107–118, 1981

4. Fukui Y, Smith NT: Interactions among ventilation, the circulation, and the uptake and distribution of halothane—Use of a hybrid computer multiple model: II. Spontaneous *vs.* controlled ventilation and the effects of CO_2. ANESTHESIOLOGY 54:119–124, 1981

5. Eger EI II: Anesthetic Uptake and Action. Baltimore, Williams and Wilkins, 1974, p 230

6. Coburn CM, Eger EI III: The partial pressure of isoflurane or halothane does not affect their solubility in blood: Inhaled anesthetics obey Henry's law. Anesth Analg 65:672–674, 1986

7. Miller KW: Specific and nonspecific actions of general anesthetic agents, Effects of Anesthesia. Edited by Covino BG, Fozzard HA, Rehder K, Strichartz G. Bethesda, American Physiological Society, 1985, pp 29–38

8. Ueda I, Kamaya H: Molecular mechanisms of anesthesia. Anesth Analg 63:929–945, 1984

9. Godfrey K: Compartmental Models and Their Application. New York, Academic Press, 1983

10. Trudell JR, Hubbell WL: Localization of molecular halothane in phospholipid bilayer model nerve membranes. ANESTHESIOLOGY 44:202–205, 1976

11. Cahalan MK, Litt L, Botvinick EH, Schiller NB: Advances in noninvasive cardiovascular imaging: Implications for the anesthesiologist. ANESTHESIOLOGY 66:356–372, 1987

12. Litt L, González-Méndez R, Severinghaus JW, Hamilton WK, Shuleshko J, Murphy-Boesch J, James TL: Cerebral intracellular changes during supercarbia: An in-vivo ^{31}P nuclear magnetic resonance study in rats. J Cereb Blood Flow Metab 5:537–544, 1985

13. Bendall MR, Gordon RE: Depth and refocusing pulses designed for multipulse NMR with surface coils. J Magn Reson 53:365–385, 1983

14. Bendall MR: Surface coils and depth resolution using the spatial variation of radiofrequency field, Biomedical Magnetic Resonance. Edited by James TL, Margulis AR. San Francisco, Radiology Research and Education Foundation, 1984, pp 99–126

15. Evelhoch JL, Ackerman JJH: NMR T_1 measurements in inhomogeneous B_1 with surface coils. J Magn Reson 53:52–64, 1983

16. Markley JL, Horsley WJ, Klein MP: Spin-lattice relaxation measurements in slowly relaxing complex spectra. J Chem Phys 55:3604–3605, 1971

17. Moore RR, Brown T, Burt CT, Roberts MR: In-vivo ^{19}F nmr studies of halothane in rat tissues. Book of Abstracts, Society of Magnetic Resonance in Medicine, Fourth Annual Meeting, 1985, p 510

18. Cohen EN: Metabolism of halothane-2 ^{14}C in the mouse. ANESTHESIOLOGY 31:560–565, 1969

19. Cohen EN, Chow KL, Mathers L: Autoradiographic distribution of volatile anesthetics within the brain. ANESTHESIOLOGY 37:324–331, 1972

20. González-Méndez R, Moseley ME, Murphy-Boesch J, Chew WM, Litt L, James TL: Selective inversion with surface coils. Use of depth pulses for the inversion-transfer experiment in vivo. J Magn Reson 65:516–521, 1985

21. Wahrenbrock EA, Eger EI, Laravuso RB, Maruschak G: Anesthetic uptake—Of mice and men (and whales). ANESTHESIOLOGY 40:19–23, 1974

22. Koehler LS, Fossel ET, Koehlet KA: Halothane fluorine-19 nuclear magnetic resonance in dipalmitoylphosphatidylcholine liposomes. Biochemistry 16:3700–3707, 1977

23. James TL, Margulis AR: Historical development of biomedical magnetic resonance, Biomedical Magnetic Resonance. Edited by James TL, Margulis AR. San Francisco, Radiology Research and Education Foundation, 1984, pp 1–6

24. Joseph PM, Fishman JE, Mukherji B, Sloviter HA: In vivo ^{19}F nmr imaging of the cardiovascular system. J Comput Assist Tomogr 9:1012–1019, 1985

25. Longmaid HE III, Adams DF, Neirinckx RD, Harrison CG, Brunner P, Seltzer SE, Davis MA, Neuringer L, Geyr RP. In vivo ^{19}F imaging of liver, tumor, and abscess in rats. Invest Radiol 20:141–145, 1985

26. McFarland E, Koutcher JA, Rosen BR, Teicher B, Brady TJ. In vivo ^{19}F imaging. J Comput Assit Tomogr 9:8–15, 1985.

27. Burt CT, Moore RR, Roberts MF, Brady TJ: The fluorinated anesthetic halothane as a potential nmr biologic probe. Biochim Biophys Acta 805:375–381, 1984

28. Wyrwicz AM, Li Y-E, Burt CT: Multiple environments of fluorinated anesthetics in intact tissues observed with ^{19}F NMR spectroscopy. FEBS Lett 162:334–338, 1983

29. Chew WM, Moseley ME, Mills PA, Sessler D, González-Méndez R, James TL, Litt L: Spin-echo fluorine magnetic resonance imaging at 2 tesla; In vivo spatial distribution of halothane in the rabbit head. Magn Reson Imaging 5:51–56, 1987

30. Budinger TF, Margulis AR: Medical Magnetic Resonance Imaging and Spectroscopy—A Primer. Berkeley, Society of Magnetic Resonance in Medicine, 1986

31. Fukishima E, Roeder SB: Experimental Pulse NMR. Reading, Addison-Wesley, 1981, pp 1–46

32. Bendall MR: Surface coil techniques for in vivo NMR. Bulletin of Magnetic Resonance 8:17–42, 1986